

# **Preparation of Anode-electrolyte Structures Using Graphite, Sodium Bicarbonate or Citric Acid as Pore Forming Agents for Application in Solid Oxide Fuel Cells**

R. da Paz Fiuza, M.A. da Silva, B.C. Guedes, L.A. Pontes, J.S. Boaventura

This document appeared in

Detlef Stolten, Thomas Grube (Eds.):

18th World Hydrogen Energy Conference 2010 - WHEC 2010

Parallel Sessions Book 1: Fuel Cell Basics / Fuel Infrastructures

Proceedings of the WHEC, May 16.-21. 2010, Essen

Schriften des Forschungszentrums Jülich / Energy & Environment, Vol. 78-1

Institute of Energy Research - Fuel Cells (IEF-3)

Forschungszentrum Jülich GmbH, Zentralbibliothek, Verlag, 2010

ISBN: 978-3-89336-651-4

# Preparation of Anode-electrolyte Structures Using Graphite, Sodium Bicarbonate or Citric Acid as Pore Forming Agents for Application in Solid Oxide Fuel Cells

**Raigenis da Paz Fiuza\***, Marcos Aurélio da Silva, Bruna C. Guedes, Luiz A. Pontes, Jaime Soares Boaventura, Energy and Materials Science Group, GECIM, Institute of Chemistry, Physical Chemistry Department, UFBA, 41170290, Salvador, Bahia, Brazil

## Abstract

Cermets based on Ni supported on YSZ or GDC were prepared for use as anode in direct reform SOFCs.  $\text{NaHCO}_3$  (Na-Ni-YSZ and Na-Ni-GDC) or citric acid (Ac-Ni-YSZ and Ac-Ni-GDC) were used as pore forming agents (PFAs). The SOFC anode was also prepared using graphite (G-Ni-YSZ and G-Ni-GDC) as PFA for the purposes of comparison. The testing unitary SOFC, planar type, was made by pressing the anode-electrolyte assembly, followed by sintering at 1500 °C. After this, LSM (lanthanum and strontium manganite) paint was used for the cathode deposition. The powdered cermets were evaluated in ethanol steam reforming at 650 °C. The ethanol conversion was 84% and 32% for cermets Na-Ni-YSZ and G-Ni-YSZ, respectively and the selectivity to  $\text{H}_2$  was 32% and 20% for the two cermets, respectively. The Na-Ni-YSZ cermet was ten times more resistant to carbon deposition than the G-Ni-YSZ cermet. SEM micrographs of the anode-electrolyte assembly showed that the use of  $\text{NaHCO}_3$  as PFA created a well formed interface between layers with homogeneously distributed pores. In contrast, graphite as PFA formed a loose interface between anode and electrolyte. The performance of the unitary SOFC was evaluated using ethanol, hydrogen or methane as fuel. The cell operated well using any of these fuels; however, they exhibited different electrochemical behavior.

**Keywords:** SOFC, cermet, pore forming agent (PFA), YSZ, GDC, ethanol, methane

## 1 Introduction

In recent years, there has been a significant increase in research into new energy sources, especially focused on the production of clean energy. In this search for alternative sources, solid oxide fuel cells (SOFC) have been one of the highlights, offering an excellent option for the clean production of energy. They have therefore attracted great technological interest, especially for their capacity to handle almost any fuel. These cells can operate with pure  $\text{H}_2$ , but their cost is greatly minimized when they operate with hydrocarbon or ethanol directly reformed on the anode [1, 2].

SOFCs basically consist of three components: First, the electrolyte is composed of a dense material conductor of  $\text{O}^{2-}$  species. Second, the anode is usually made of a metallic electro-catalyst supported on the same (or similar) material used as electrolyte. Third, the cathode is

---

\* Corresponding author, email: raigenis@ufba.br

also an electro-catalyst of porous structure whose main task is to reduce oxygen and it usually consists of mixed oxides [3-6]. The performance of SOFCs strongly depends on the component microstructure, especially the anode structure [7], which should be well adhered to the electrolyte, making available paths for conducting oxygen ions to enlarge the boundary region of the triple phase. The anode must also have adequate porosity, around 40%, to allow a good fuel distribution, as well as a good dispersion of the metal phase on the support. The metal particle size distribution must be adequate to form a continuous metallic phase on the support, making the anode an electrical conductor [8]. This paper studies the construction and evaluation of the microstructure of an anode-electrolyte set as well as the catalytic activity of the anode, both produced using different pore forming agents (PFA): graphite,  $\text{NaHCO}_3$  and citric acid. The microstructure was studied by means of scanning electron microscopy (SEM); the anode catalytic activity was evaluated for ethanol steam reforming.

## 2 Methodology

The preparation of anode-electrolyte set was made using graphite,  $\text{NaHCO}_3$  or citric acid as PFA. The electrolyte was produced from YSZ (8 mol-%  $\text{Y}_2\text{O}_3$  in  $\text{ZrO}_2$ ) and GDC ( $\text{Gd}_{0.1}\text{Ce}_{0.9}\text{O}_2$ ); the three PFAs were used with both materials. First, a mixture of YSZ, graphite and NiO was prepared to produce the anode [9, 10], formulate to contain 35% by weight of Ni metal and enough graphite to generate an average porosity of 40%. The electrolyte was formed with pure YSZ; a layer of the previous described mixture (as anode) and a layer of pure YSZ (as electrolyte) were put into a steel mold and pressed to produce pellets of an average thickness of one millimeter. This set based on YSZ, NiO and graphite was called G-Ni-YSZ. The same procedure was reproduced, replacing YSZ, both in the electrolyte and anode, by GDC; the set was named G-Ni-GDC. The sets were synthesized according to a careful heating program, taking into account the temperature of melting, boiling and decomposition of PFA and Na derivatives formed during the sintering in air, up to a temperature of 1500 °C for effective sintering. The samples were characterized by Scanning Electron Microscope (SEM) techniques and the average porosity was measured by water absorption.

To evaluate the effect of residual Na on the electro-catalyst, two cermets were prepared. For the first one, NiO, YSZ (8%  $\text{Y}_2\text{O}_3$  in  $\text{ZrO}_2$ ) and graphite (as PFA) were mechanically mixed and sintered at 1400 °C. This cermet was named G-Ni-YSZ. The other cermet was prepared in a similar fashion, however, the graphite was replaced by  $\text{NaHCO}_3$ ; this cermet was named Na-Ni-YSZ. The Ni contents of both cermets were around 35% in mass. After sintering, the cermets were reduced to powder and separated in a 300 mesh sieve. They were evaluated in ethanol steam reforming at 650 °C in a quartz flow reactor and the reaction products were analyzed by gas chromatography. For the unitary SOFC preparation, the anode (Na-Ni-YSZ) and electrolyte were similarly pressed in a steel mould and sintered at 1500 °C for 3 hours. Afterwards, the cathode was prepared by adding a thin layer of LSM ink and sintered at 1200 °C for one hour. Platinum screens, set on both sides of the cell by ink platinum, were used as the electrical contact. Platinum wires were used to connect the cell terminals to the circuit test. A high temperature ceramic bond was used to fix the cell to an alumina tube

which supplied fuel and oxygen to the cell. The system was put into a controlled temperature furnace and the cell was tested at 800 °C using ethanol, methane or H<sub>2</sub> as fuel.

### 3 Results and Discussion

The dense aspect of the samples seen in the microphotographs indicated that they reached a high degree of densification, as Figure 1 shows. Additional SEM microphotographs revealed the good densification of GDC electrolyte, showing that the temperatures used were appropriate for its sintering. As noted in the literature, YSZ can be well sintered at lower temperatures, around 1350-1400 °C, however, GDC requires a higher sintering temperature, around 1450 °C [4, 9, 10]. For all the SOFCs prepared in this work, the electrolytes had an average thickness of 150 to 200 µm and the anodes were 400 µm thick, measured using SEM techniques.

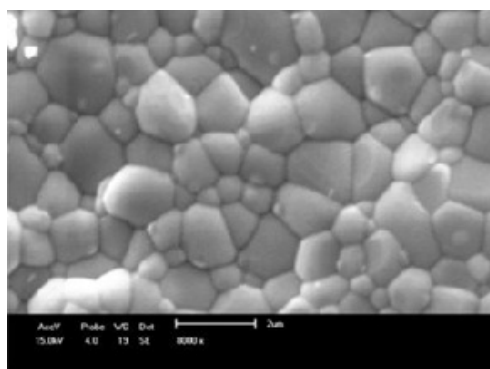
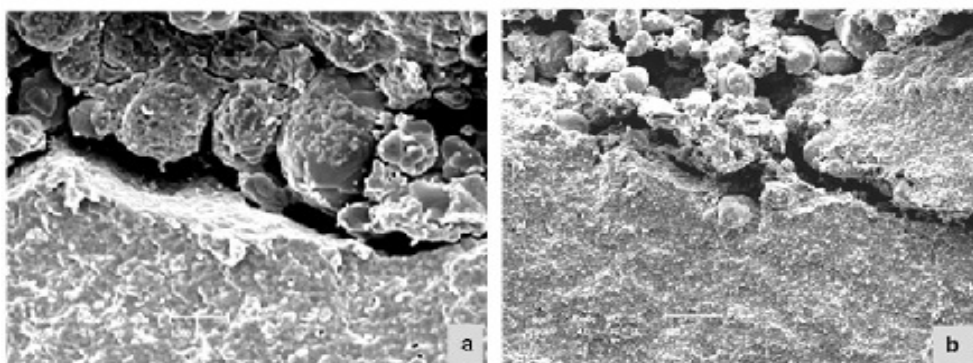


**Figure 1:** SEM image obtained from fracture region of AC-Ni-GDC electrolyte sample after sintering at 1500 °C.

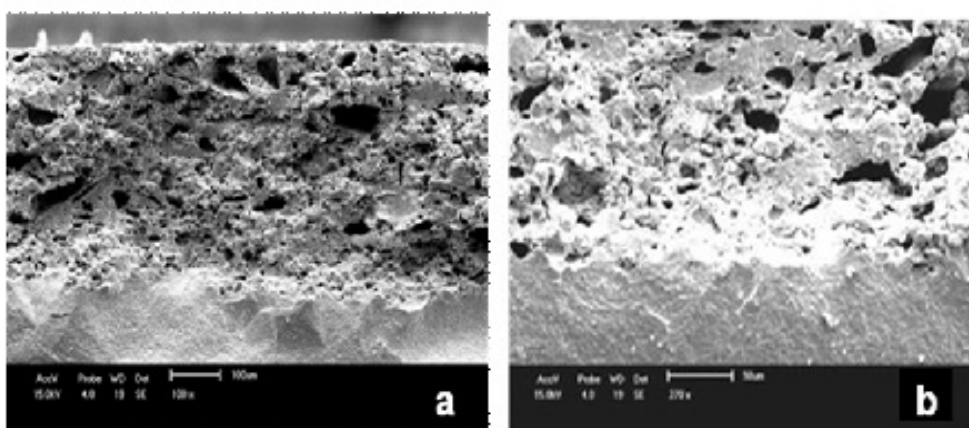
The micrographs in Figure 2 show that the use of graphite as a PFA led to the formation of well distributed pores over the anode; they were uniform and connected to each other. However, the graphite apparently induced a separation of anode and electrolyte layers, weakening the interface and allowing these layers to come easily apart. This separation between anode and electrolyte was probably related to the lubricant action of graphite, preventing good adhesion between the anode and electrolyte layers; therefore the anode-electrolyte interface formed discontinuities during the sintering process [11]. The separation between anode and electrolyte probably reduced the number of available passes of oxygen ions [3].

The addition of NaHCO<sub>3</sub> or citric acid to the anode as PFAs led to the formation of pores with the same characteristics as observed in samples prepared with graphite, i.e. pores well distributed over the anode, uniform and connected to each other. However, excellent connectivity between anode-electrolyte, for both Na-Ni-YSZ and Ac-Ni-YSZ samples, was observed, as may be seen in Figures 3 and 4. The good adherence between anode-electrolyte layers for pellets made using NaHCO<sub>3</sub> as a PFA may be attributed to the formation of a liquid phase during heating due to the formation of sodium hydroxide and oxide [12]. This liquid phase served as a bonding agent and promoted such a good adhesion

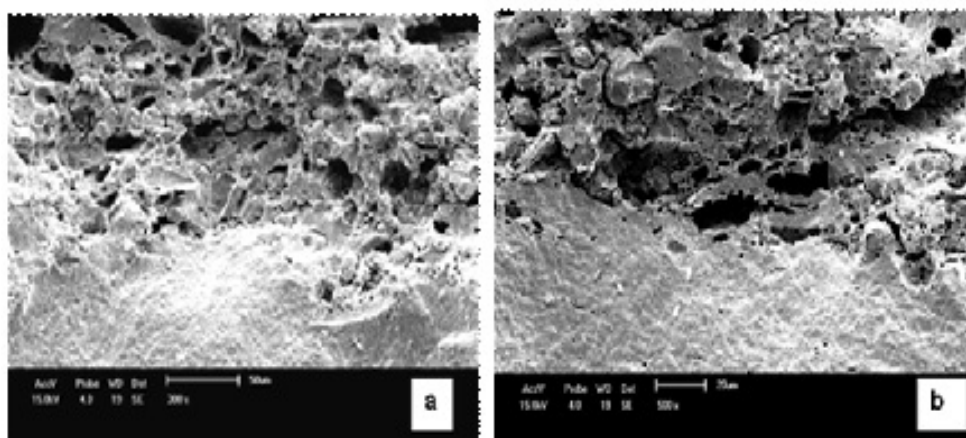
between anode and electrolyte layers that they formed a single block. Furthermore, pellets made with citric acid as a PFA showed adherence as good as those made with sodium [13].



**Figure 2:** SEM image obtained from the electrolyte-anode interface of fractures – a) G-Ni-YSZ; b) G-Ni-GDC – both samples after sintering at 1500 °C (1220x magnification).

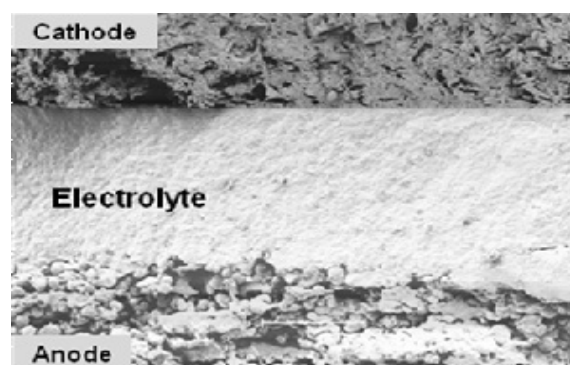


**Figure 3:** SEM image of the electrolyte-anode interface: a) Na-Ni-YSZ and b) Na-Ni-GDC.



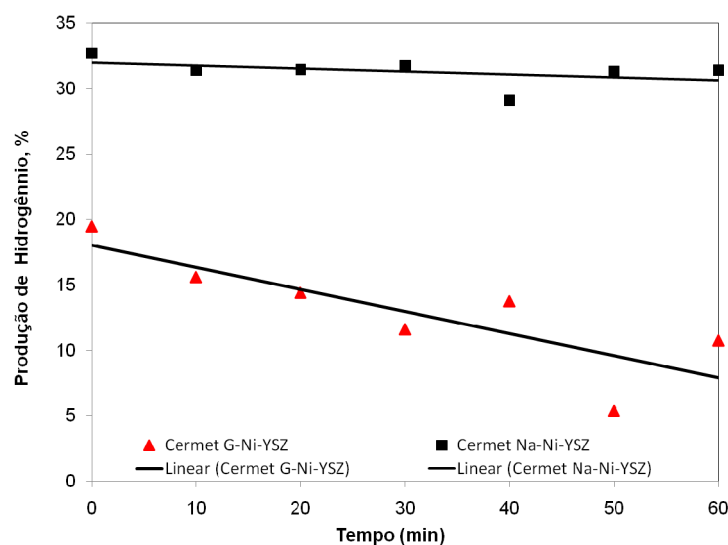
**Figure 4:** SEM image of the electrolyte-anode interface: a) Ac-Ni-YSZ and b) Ac-Ni-GDC.

Figure 5 shows a SEM micrograph of the anode-electrolyte-cathode assembly used for the unitary SOFC test. The anode-electrolyte-cathode interfaces were well constructed and did not present any discontinuity. Well constructed interfaces are fundamental for the performance of the cell in electricity generation [14]. Müller et al. [15], investigating electrode (cathode and anode) and electrolyte interfaces, reached the same conclusion regarding the fundamental role of interfaces on unitary SOFC performance. Furthermore, Weber and Ivers-Tiffée [16] demonstrated that the penetration of the electrolyte phase into the electrode phase significantly lowered the cell ohmic resistance. On the other hand, discontinuity regions at the interfaces drastically reduced the performance of the cell [17].



**Figure 5: SEM image obtained from the cathode-electrolyte-anode interface of a fracture of Na-Ni-YSZ samples after sintering at 1500 °C.**

The results of the catalytic test, carried out for the steam reforming of ethanol at 650 °C, showed that the Na-Ni-YSZ cermet was more active than the G-Ni-YSZ sample. The ethanol conversion increased by a factor of 2.5 and the H<sub>2</sub> production increased almost twofold. These tests also indicated that the relative amount of deposited carbon for the Na-Ni-YSZ cermet was around ten times lower than the carbon formation on the G-Ni-YSZ cermet. This significant reduction in carbon formation was attributed to the lower acidity of the Na-Ni-YSZ sample due to the basic effect of Na species formed during the cermet sintering. These results are in agreement with Haryanto et al. and Llorca et al. [18, 19]. They observed that the reduction in acidity of the catalyst was beneficially reflected in reducing the formation of carbon deposits which contributed to the deactivation of the catalyst when the cells were fed directly with gaseous ethanol. In addition to the higher activity of Na-Ni-YSZ, this electro-catalyst was more stable than the G-Ni-YSZ cermet during the studied reaction period. These results may be seen in Figure 6. The figure presents the H<sub>2</sub> concentration profile obtained during the test for carbon deposition. The reaction was carried out for one hour and Na-Ni-YSZ lost around 2% of its activity, while G-Ni-YSZ deactivated by around 17%. The improved stability of Na-Ni-YSZ is in agreement with results reported by Frusteri et al. [20], who noticed lower deactivation of electro-catalysts with lower acidity.



**Figure 6: H<sub>2</sub> production from the steam reforming of ethanol at 650 °C, measured as molar concentration at the reactor outlet. The reaction was carried out for one hour.**

The unitary SOFC has been tested with H<sub>2</sub>, gaseous ethanol or methane; the performance of the SOFCs with the various fuels is shown in Figures 7 to 9. The power delivered by the cell increased with the fuel used in the following order: H<sub>2</sub> < ethanol < methane. The differences in the cell behavior with the various fuels may be explained on the basis of H<sub>2</sub> species availability on the triple phase boundary (TPB). The adsorbed H<sub>2</sub> species were readily available from the methane or ethanol reforming, while adsorption and dissociation steps were required for gaseous H<sub>2</sub>. This variation in the cell performance with the fuel used may be better seen from the potential and over-potential versus current curves, shown in Figures 8 and 9, respectively. The potential curve profile for ethanol, with a steep over potential variation at low current, suggest that the anode concentration polarization was the dominant term for the ethanol cell over-potential [22, 23]. This term may arise from the lower diffusivity of gaseous ethanol. Following the low current regime, the over-potential was very closely linear to the current for all three fuels. This linearity of the over-potential has been associated with the activation and ohmic polarizations of the cell [24, 25]. The linear coefficient of the over-potential dependence on cell current increased with the fuel used as follows: ethanol < methane < H<sub>2</sub>. This order is in agreement with the above reasoning that H<sub>2</sub> adsorption and dissociation were significant kinetic steps in H<sub>2</sub> oxidation; Ye et al. [26] made a similar observation. Furthermore, if one assumes that activation polarization are negligible for the ethanol over potential, the cell ohmic polarization was comparable to the cell activation polarization with methane and half the value with H<sub>2</sub> [24]. The results suggested that the cell resistance due to the electrolyte layer and its interfaces was relatively low, indicating that the NaHCO<sub>3</sub> used as PFA was an excellent alternative.

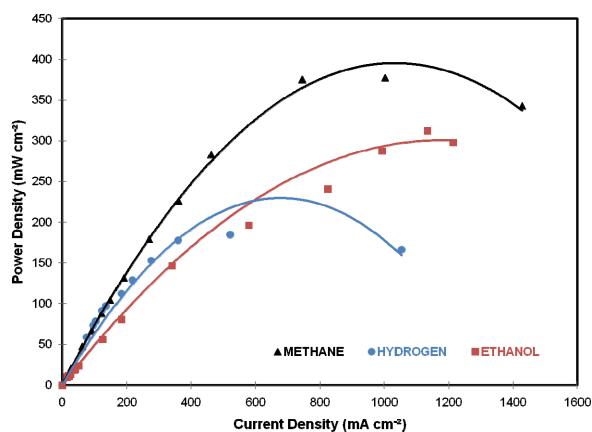


**Figure 7:** Performance of unitary test SOFC operating at 800 °C.

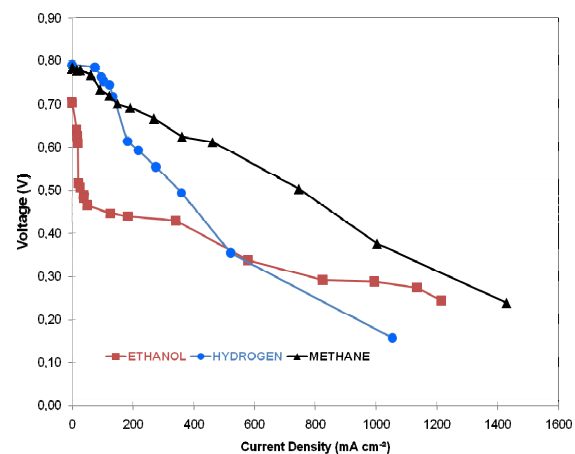


**Figure 8:** Cell potential versus current density for the unitary test SOFC operating at 800 °C.

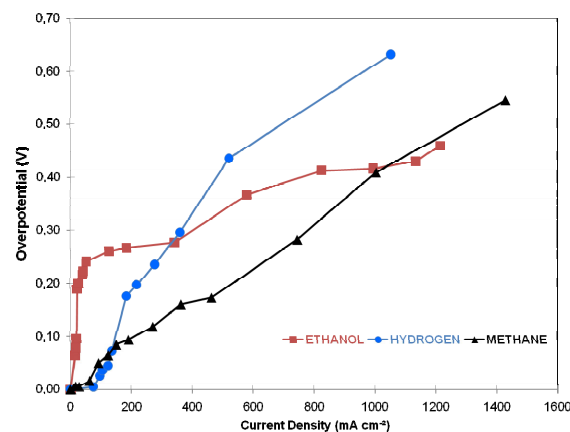


**Figure 9:** Cell over-potential versus current density for the unitary test SOFC operating at 800 °C.

#### 4 Conclusion

The results show that the temperature of 1500 °C is well suited to the promoting of good sintering of GDC and YSZ pellets. Lower temperatures may sinter YSZ, but not GDC.  $\text{NaHCO}_3$ , citric acid and graphite have similar characteristics in the formation of coalescing, connected and well distributed pores. However,  $\text{NaHCO}_3$  and citric acid, unlike graphite, enables strong adhesion of the interface between anode and electrolyte, forming a compact block which is a very important feature for high efficiency SOFCs. Furthermore, the cermet prepared with  $\text{NaHCO}_3$  presented higher activity for ethanol steam reforming and around a ten times lower tendency for carbon deposition in comparison with the cermet prepared with graphite. The unitary SOFC prepared with an anode using  $\text{NaHCO}_3$  as a pore forming agent shows low internal ohmic resistance for all the fuels tested ( $\text{H}_2$ , ethanol and methane),



indicating very high ionic conductance of the anode-electrolyte interface. These aspects contribute significantly to the technological advancement in the development of fuel cell components, overcoming one of the major barriers to increasing cell efficiency by the reduction of the ohmic resistance of the device.

### Acknowledgments

The authors gratefully acknowledge grants from the Brazilian Ministry of Science and Technology (MCT) to support this work. They are particularly grateful to Rede PaCOS (grant 01.06.0901.00) and Rede Norte/Nordeste de Catálise (RECAT, grant 22.02.0289.00), supported by FINEP/CT-PETRO. The authors also acknowledge FAPESB (MAS) and CNPq (RPF) for their helpful scholarships.

### References

- [1] A. B. Stambouli, E. Traversa, *Renew. Sust. Energ. Rev.*, 6 (2002) 433.
- [2] A. Atkinson, S. Barnett, R. J. Gorte, J. T. S. Irvine, A. J. McEvoy, M. Mogensen, S. C. Singhal, J. Vohs, *Nature Mater.*, 3 (2004) 17.
- [3] D. Z. de Florio, F. C. Fonseca, E. N. S. Muccillo, R. Muccillo, *Cerâmica*, 50 (2004) 275.
- [4] J. B. Goodenough, *Annu. Rev. Mater. Sci.*, 33 (2003) 91.
- [5] K. Chen, Z. Lü, X. Chen, N. Ai, X. Huang, B. Wei, J. Hu, W. Su, *J. Alloys Compd.*, 454 (2008) 447.
- [6] R. S. Amado, L. F. B. Malta, F. M. S. Garrido, M. E. Medeiros, *Química Nova*, 30 (2007) 189.
- [7] J.-H. Lee, J.-W. Heo, D.-S. Lee, J. Kim, G.-H. Kim, H.-W. Lee, H. S. Song, J.-H. Moon, *Solid State Ionics*, 158 (2003) 225.
- [8] R. J. Gorte, J. M. Vohs, *J. Catal.*, 216 (2003) 477.
- [9] M. A. Silva, M. G. F. Alencar, R. P. Fiuza, J. S. Boaventura, *Revista Matéria*, 12 (2007) 72.
- [10] M. A. Silva, J. S. Boaventura, M. G. Alencar, C. P. Cerqueira, *Revista Matéria*, 12 (2007) 99.
- [11] H. Yu, P. Hu, T. Shang, M. Jiang, Q. Chen, *J. Wuhan Univ. Technol. - Mater. Sci. Ed.*, 23 (2008) 130.
- [12] A. S. Maia, V. K. L. Osorio, *Química Nova*, 26 (2003) 595.
- [13] J. Zhao, X. Liu, L. Qiang, *Thin Solid Films*, 515 (2006) 1455.
- [14] A. McEvoy in S.C. Singhal, K. Kendall (Eds.). Elsevier, Netherlands, 149-171, 2003.
- [15] A. C. Müller, D. Herbstritt, E. Ivers-Tiffée, *Solid State Ionics*, 152 (2002) 537.
- [16] A. Weber, E. Ivers-Tiffée, *J. Power Sources*, 127 (2004) 273.
- [17] Y. L. Liu, S. Primdahl, M. Mogensen, *Solid State Ionics*, 161 (2003) 1.
- [18] A. Haryanto, S. Fernando, N. Murali, S. Adhikari, *Energ. Fuel.*, 19 (2005) 2098.
- [19] J. Llorca, N. Homs, J. Sales, J. L. G. Fierro, P. R. de la Piscina, *J. Catal.*, 222 (2004) 470.
- [20] F. Frusteri, S. Freni, Chiodo L. Spadaro, O. D. Blasi, G. Bonura S. Cavallaro, *Appl. Catal. A*, 270 (2004) 1.

- [21] J. R. Rostrup-Nielsen, L.J. Christiansen, Appl. Catal. A, 126 (**1995**) 381.
- [22] W. Z. Zhu, S. C. Deevi, Mater. Sci. Eng. A 362 (**2003**) 228.
- [23] S. H. Chan, K. A. Khor, Z. T. Xia, J. Power Sources, 93 (**2001**) 130.
- [24] M. Ni, M. K.H. Leung, D. Y. C. Leung, Energy Convers. Manage., 48 (**2007**) 1525.
- [25] W. G. Bessler, S. Gewies, M. Vogler, Electrochim. Acta, 53 (**2007**) 1782.
- [26] X. F. Ye, S. R. Wang, Z. R. Wang, L. Xiong, X. F. Sun, T. L. Wen, J. Power Sources, 177 (**2008**) 419.